Drug/Dye-Loaded, Multifunctional Iron Oxide Nanoparticles for Combined Targeted Cancer Therapy and Dual Optical/Magnetic Resonance Imaging

*Santimukul Santra, Charalambos Kaittanis, Jan Grimm, and J. Manuel Perez**

***A** biocompatible, multimodal, and theranostic functional iron oxide nanoparticle is synthesized using a novel water-based method and exerts excellent properties for targeted cancer therapy, and optical and magnetic resonance imaging. For the first time, a facile, modified solvent diffusion method is used for the co-encapsulation of both an anticancer drug and near-infrared dyes. The resulting folate-derivatized theranostics nanoparticles could allow for targeted optical/magnetic resonance imaging and targeted killing of folate-expressing cancer cells.*

Keywords:
- click chemistry
- drug delivery
- magnetic materials
- magnetic resonance imaging

1. Introduction

Superparamagnetic iron oxide nanoparticles with dual imaging and therapeutic capabilities hold great promise for the noninvasive detection and treatment of tumors.[1] When conjugated with tumor-specific targeting ligands, these multifunctional nanoparticles can be used to specifically deliver anticancer drugs to tumors, thereby minimizing severe side effects.[2] To meet the demand for the rapid development and potential clinical application of targeted anticancer nanotherapies, it is desirable to introduce optical (fluorescent) imaging capabilities to these nanoparticles to facilitate noninvasive assessment of drug homing and efficacy. This is often achieved by crosslinking the polymeric coating surrounding the nanoparticle and functionalizing its surface with amine or carboxyl groups that are then used to conjugate fluorescent dyes and drugs.[3] This approach to introduce multimodality (magnetic and fluorescent)[4] and multifunctionality (imaging and therapeutic)[5] to iron oxide nanoparticles (IONPs), although widely used, often compromises the solubility of the nanoparticles in aqueous media and reduces the number of available functional groups that otherwise could be used to attach ligands for targeting applications.

Herein, we report the co-encapsulation of a lipophilic near infrared (NIR) dye and an anticancer drug within hydrophobic pockets in the polymeric matrix of poly(acrylic acid) (PAA)-coated IONPs (PAA-IONPs) for combined optical imaging, magnetic resonance imaging (MRI) detection, and targeted cancer therapy. Our water-based and green chemistry approach to synthesize these nanoparticles has five key components: i) an encapsulated chemotherapeutic agent (Taxol) for cancer therapy, ii) surface functionality (folic acid ligand) for cancer targeting, iii) click-chemistry-based conjugation of targeting ligands, iv) an encapsulated NIR dye for fluorescent imaging capabilities, and v) a superparamagnetic iron oxide core for MRI.

2. Results and Discussion

Our synthetic procedure differs from the previously reported methods in that the polymer is not present during the initial nucleation process.[6–8] Instead, the PAA is added at a later stage. This step-wise process, as opposed to the in situ process, allows for the formation of stable, disperse, and highly crystalline superparamagnetic iron oxide nanocrystals coated with PAA (**1**, Scheme 1). The successful coating with PAA was confirmed by the presence of a negative zeta-potential ($\zeta = -48$ mV) and via Fourier transform infrared spectroscopy (FTIR) analysis (see Supporting Information 5). We then hypothesized whether a hydrophobic dye could be encapsulated

[*] Dr. J. M. Perez, Dr. S. Santra, C. Kaittanis
Nanoscience Technology Center, Chemistry Department
Burnett School of Biomedical Sciences, College of Medicine
University of Central Florida
12424 Research Parkway, Suite 400, Orlando, FL 32826 (USA)
E-mail: jmperez@mail.ucf.edu
Dr. J. Grimm
Department of Radiology, Memorial Sloan Kettering Cancer Center
1275 York Avenue New York, NY 10065 (USA)

Supporting information for this article is available on the WWW under http://www.small-journal.com or from the author.

DOI: 10.1002/smll.200900389

WILEY InterScience DISCOVER SOMETHING GREAT

© 2009 Wiley-VCH Verlag GmbH & Co. KGaA, Weinheim

NANO MICRO small

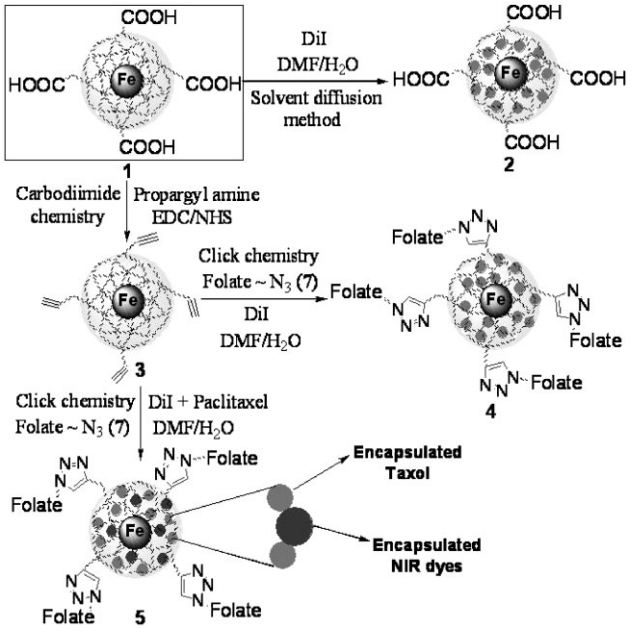

Scheme 1. Schematic representation of the synthesis of theranostics and multimodal IONPs. Click chemistry and carbodiimide chemistry have been used for the synthesis of a library of functional IONPs. NIR dyes and paclitaxel co-encapsulated IONPs were prepared in water using the modified solvent diffusion method (see Supporting Information 1 and 2 for detailed synthetic procedures).

within the hydrophobic pockets in the PAA coating, generating multimodal IONPs with dual magnetic and fluorescent properties. As a proof-of-principle, we have encapsulated two lipophilic fluorescent dyes (DiI or DiR) (**2**, Scheme 1) using a modified solvent diffusion method.[9] These dialkylcarbocyanine fluorophores (DiI, DiR) are widely used in biomedical applications to label cell membranes and were selected because of their high extinction coefficients ($\varepsilon > 125\,000\,cm^{-1}\,M^{-1}$) and high fluorescence in hydrophobic environments.[9] The long chain dialkylcarbocyanine dye, DiR, is of particular importance since it has an excitation/emission near the infrared region (751/780 nm), suitable for in vivo imaging.

Next, the IONP **1** was functionalized to yield a propargylated nanoparticle (**3**, Scheme 1), which was later used to generate a multimodal folate-derivatized nanoparticle (**4**, Scheme 1) via highly selective 1,3-dipolar cycloaddition reaction (click chemistry).[10] Thus, the water-soluble carbodiimide EDC, [1-ethyl-3-(3-dimethylaminopropyl) carbodiimide hydrochloride] was utilized to prepare the propargylated IONP (**3**, Scheme 1), which is an important synthon for the synthesis of a library of functional IONPs via click chemistry. The presence of a weak "C=C" band at 2265 cm^{-1} in the FTIR spectrum of these nanoparticles confirmed the presence of a propargyl (triple bond) group (see Supporting Information 6). As a model system, we conjugated the nanoparticle **3** with an azide-functionalized folic acid[11] analog (see Supporting Information 1 and 2) via click chemistry. The resulting folate-decorated IONPs are soluble in aqueous media and can encapsulate lipophilic fluorescent dyes. The presence of folic acid and dye in these multimodal folate-derivatized nanoparticles (**4**, Scheme 1) was confirmed through various spectrophotometric studies (see Supporting Information 7, 8, and 9). Furthermore, a hydrophobic anticancer drug (Taxol) was encapsulated to yield a theranostic (therapeutic and diagnostic) nanoparticle with dual imaging and therapeutic properties (**5**, Scheme 1). These functional IONPs (**1**–**5**) were highly stable in aqueous solutions, as their magnetic relaxivity (R_2), hydrodynamic diameter (D), and polydispersity index (PDI) remained unaffected over a long period of time (see Supporting Information 3). Therefore, the versatility of our method allows the generation of a small library of multifunctional, multimodal, and targetable IONPs.

Dynamic light scattering (DLS) studies of the functional PAA-IONP (**2**) confirmed the presence of stable and monodisperse nanoparticles with a D of 90 nm (Figure 1A), while transmission electron microscopy (TEM) experiments revealed an iron oxide core of 8 nm (inset, Figure 1A; see Supporting Information 4). These measurements suggest the formation of a thick polymeric coating (≈40 nm) around the iron oxide core, which plays a key role in the encapsulation of hydrophobic guest molecules. FTIR analysis further confirmed the presence of the PAA coating and carboxylic acid groups on **1**, as well as the corresponding surface propargyl

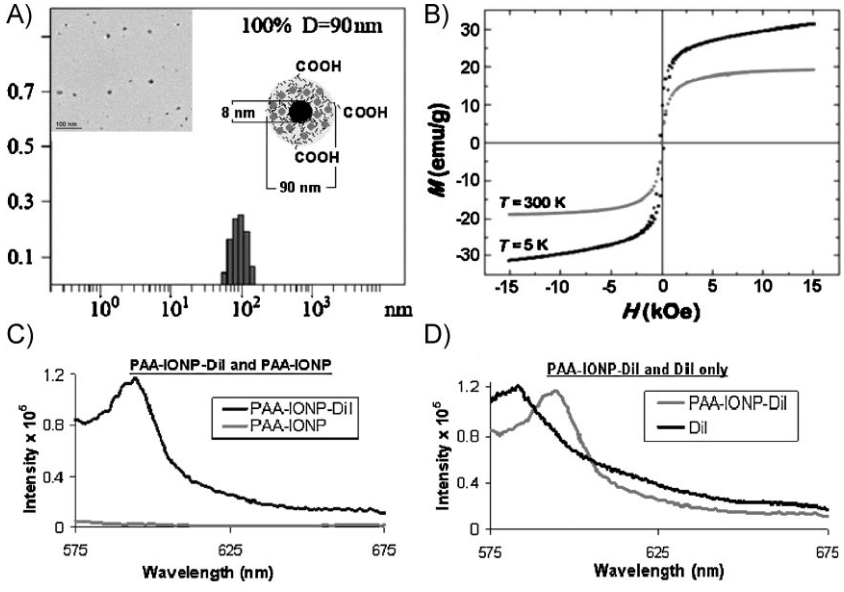

Figure 1. Characterization of multimodal nanoparticles **2** (PAA-IONP-DiI). A) Determination of D of the IONPs through DLS. Inset: TEM image of the corresponding nanoparticles. Scale bar 100 nm. B) Magnetic hysteresis loops at 300 and 5 K, showing nanoparticles are superparamagnetic. C) Fluorescence emission spectra (in PBS buffer) of DiI dye encapsulated IONPs **2** and that of **1** without any dye. D) Fluorescence emission spectra of **2** and that of free non-encapsulated DiI in solution.

 © 2009 Wiley-VCH Verlag GmbH & Co. KGaA, Weinheim

groups on nanoparticle **3** (see Supporting Information 5 and 6). Magnetic hysteresis loops (Figure 1B) corroborated the superparamagnetic nature of the nanoparticles, while water relaxation measurements using a 0.47T Bruker's Minispec relaxometer indicated the presence of magnetic IONPs with high water relaxation ($R_1 = 53\,s^{-1}\,mM^{-1}$, $R_2 = 202\,s^{-1}\,mM^{-1}$). The incorporation of a hydrophobic dye into **1** was done using a modified solvent diffusion method.[9] Specifically, a solution of DiI in dimethylformamide (DMF) ($0.1\,\mu g\,\mu L^{-1}$) was added drop-wise to a stirring aqueous nanoparticle suspension (4.5 mL and $[Fe] = 1.1\,mg\,mL^{-1}$). The slow addition of the dye solution allows for the rapid diffusion of DMF into the aqueous medium, causing the dye to become encapsulated in the hydrophobic microdomains of the PAA coating. The presence of an absorption maximum at 555 nm in the UV–Vis spectrum (see Supporting Information 8a) and a corresponding fluorescence emission peak at 595 nm (Figure 1C) confirmed the presence of DiI in the nanoparticle. Furthermore, the encapsulation of DiI was confirmed by the presence of a 14-nm red-shift in the fluorescence intensity maximum of the DiI-encapsulating PAA-IONP, as compared to the free DiI (581 nm, Figure 1D). Similar red-shifts have been previously reported in other systems, indicating an interaction of the fluorescent guest molecule with the electronic environment of the encapsulating pocket.[12] Next, we encapsulated both DiI and Taxol to the folate-conjugated nanoparticle for dual cellular imaging and targeted cancer therapy. To synthesize such a nanoparticle (**5**), a DMF solution containing DiI ($0.1\,\mu g\,\mu L^{-1}$) and Taxol ($0.05\,\mu g\,\mu L^{-1}$) was added to a stirring solution of folate-derivatized PAA-IONPs (**3a**, see Supporting Information 1). Since the dye and the drug are hydrophobic, we expected both molecules to become encapsulated. The encapsulation of Taxol was confirmed through fluorescence spectroscopy (see Supporting Information 10). Furthermore, the amount of dye, folic acid, and Taxol molecules per nanoparticle were calculated, as previously described[13] (Table 1). These dye-encapsulating PAA-IONPs were highly stable in aqueous solutions for more than a year without significant reduction in the fluorescence emission of the encapsulated dyes. Additionally, no leaching of the encapsulated dye from the nanoparticle occurred, as no precipitation of the dye was observed after prolonged storage in phosphate buffered saline (PBS), pH 7.4.

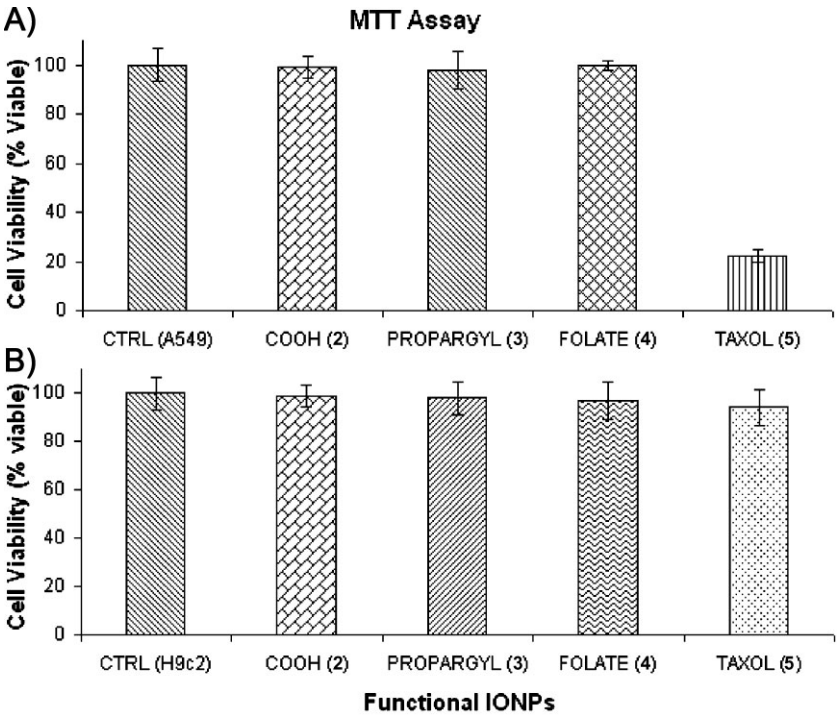

Figure 2. Determination of cytotoxicity of the functional IONPs: carboxylated [COOH (**2**)], propargylated [PROPARGYL (**3**)], folate-conjugated [FOLATE (**4**)], and Taxol-carrying [TAXOL (**5**)]. Control (CTRL) cells: A) lung carcinoma cells (A549) and B) cardiomyocyte cells (H9c2) were treated with PBS. Average values of four measurements are depicted ± standard error.

Table 1. Determination of R_2, D, and PDI of functional IONPs immediately after synthesis. Quantitative estimation of amount of dye, folic acid, and Taxol 3per iron crystal of the corresponding multifunctional IONPs (**1**–**5**).

IONPs	R_2 [$s^{-1}\,mM^{-1}$]	D (PDI) [nm]	Dye/ IONPs	Folate/ IONPs	Taxol/ IONPs
1	206 ± 2	86 ± 1 (0.89)	–	–	–
2	202 ± 3	90 ± 2 (0.87)	31 ± 2	–	–
3	207 ± 2	87 ± 1 (0.89)	–	–	–
4	204 ± 3	94 ± 3 (0.87)	28 ± 2	12 ± 2	–
5	203 ± 5	96 ± 4 (0.91)	19 ± 1	12 ± 2	11 ± 3

To evaluate the potential biomedical applications of the DiI-encapsulating IONPs (**2**, **3**, **4**, and **5**, $1.1\,mg\,mL^{-1}$), we assessed their potential cytotoxicity, via the MTT assay (Figure 2). Therefore, we examined the in vitro differential cytotoxicity of carboxylated (COOH, **2**), propargylated (PROPARGYL, **3**), folate-decorated (FOLATE, **4**), and Taxol-encapsulating IONPs (TAXOL, **5**), using lung carcinoma (A549, 2500 cells per well) (Figure 2A) and cardiomyocyte cell lines (H9c2, 2500 cells per well) (Figure 2B). Carboxylated, propargylated; and folate-conjugated IONPs exhibited nominal cytotoxicity (less than 3% compared to the control) towards both cell lines after a 3 h incubation. On the other hand, incubation with the folate-decorated and Taxol-carrying IONPs (**5**) resulted in an 80% reduction in the viability of the lung carcinoma (A549) cell line. In contrast, no significant reduction in cell viability was observed when cardiomyocytes (H9c2), which do not overexpress the folate receptor,[14] were incubated with **5**. These results demonstrate that nanoparticles **1**–**4** were not toxic to either A549 or H9c2 cells, hence these nanoparticles can be used as effective multimodal imaging agents. However, as IONP **5** was only cytotoxic to cancer cells (A549) that overexpress folate receptor,[15,16] it can be utilized as a potential targeted multifunctional (imaging and therapeutic) nanoagent for the treatment of folate-receptor-expressing tumors.

 © 2009 Wiley-VCH Verlag GmbH & Co. KGaA, Weinheim

small NANO MICRO

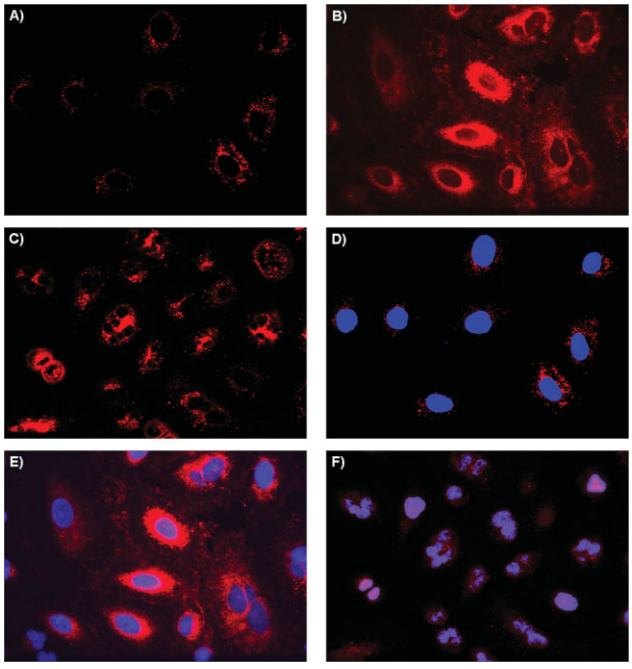

Figure 3. Assessment of IONP cellular uptake via confocal laser-scanning microscopy using lung carcinoma A549 cells. A) No internalization was observed in cells treated with carboxylated IONPs (**2**), as no DiI fluorescence was observed in the cytoplasm. B) Enhanced internalization was observed upon incubation with the folate-immobilized IONPs (**4**). C) Cells incubated with Taxol and DiI co-encapsulating folate-functionalized IONPs (**5**) induced cell death. D–F) Corresponding merged confocal images of the functional IONP-treated cells with their nucleus stained with DAPI (blue).

To further explore the potential biomedical applications of the synthesized functional PAA-IONPs, we evaluated the selective uptake of the folate-functionalized nanoparticle (**4**) by A549 lung cancer cells, as these cells overexpress the folate receptor. In these experiments, carboxylated (**2**) or folate-conjugated (**4**) nanoparticles ($1.1\,mg\,mL^{-1}$) were incubated with A549 cells (10 000 cells) for 3 h, washed to remove non-internalized nanoparticles and visualized via confocal microscopy. Results showed no internalization of the carboxylated nanoparticle (**2**) as expected (Figure 3A and D). However, significant internalization of the folate-conjugated nanoparticle (**4**) was indicated by the presence of intense fluorescence in the cytoplasm of the cells (Figure 3B and E). These results were also observed in experiments performed using live (non-fixed) A549 cells, where internalization of the folate-decorated IONPs (**4**) was monitored through fluorescence microscopy (see Supporting Information 11). The enhanced cellular uptake of the folate-decorated nanoparticle (**4**) in A549 cells may have been attributed to folate-receptor-mediated internalization. As internalization of **4** was nominal in A549 cells pre-incubated with free folate and in studies using the H9c2 cardiomyocyte cell line (see Supporting Information 12), we corroborated the receptor-mediated internalization of our folate-decorated IONPs (**4**). Next, we investigated the cellular uptake of a multifunctional folate-conjugated nanoparticle (**5**) with dual imaging and targeted cancer therapeutic properties. When these IONPs were incubated with A549 cells, mitotic arrest was observed, leading to dramatic cellular morphological changes and cell death (Figure 3C and F).

The therapeutic application of our nanoparticles depends on the rate of release of the encapsulated drug from the PAA coating. To evaluate **5**'s drug release profile, enzymatic (esterase) and low-pH degradation experiments were performed. Results indicated a fast release of the drug (Taxol) from the nanoparticle (**5**) upon esterase incubation, reaching a plateau within 2 h (Figure 4A). An even faster release of the drug was observed at pH 4.0, reaching a plateau within 30 min (Figure 4B). No significant release of the drug was observed from nanoparticles incubated in PBS (pH 7.4). These results are significant as they demonstrate the stability of the nanoparticles during storage (in PBS), and their cargo release only after cellular uptake via either esterase-mediated degradation or in acidified lysosomes. Therefore, only after its folate-receptor-mediated uptake, the nanoparticle **5** becomes cytotoxic upon intracellular release of its cargo therapeutic agent. Interestingly, a much slower release of the dye was observed, both upon esterase incubation and at pH 4.0 (Figure 4C and D). However, no release of the dye was observed at normal physiological pH (7.4). The observed differential release of the drug versus the dye from IONP **5**

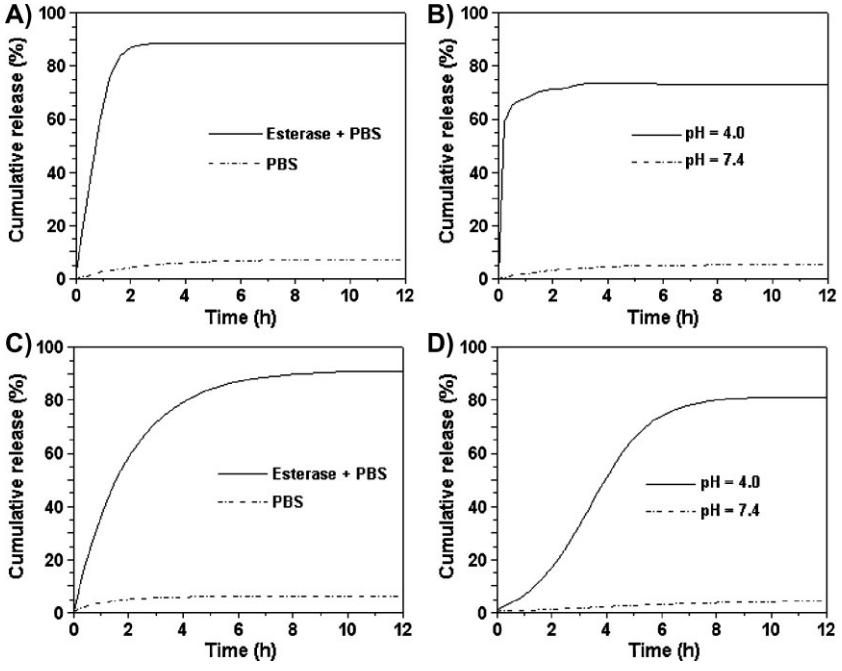

Figure 4. Drug and dye release profiles of functional IONPs (**5**) in PBS (pH 7.4) at 37 °C. Release of Taxol (A and B) and DiI (C and D) were observed in the presence of an esterase enzyme (A and C) and at pH 4.0 (B and D).

© 2009 Wiley-VCH Verlag GmbH & Co. KGaA, Weinheim

may be attributed to the drug's (Taxol) size and hydrophobic nature.

Taken together, these results make our folate-decorated IONP (**5**) an important drug carrier, as it can rapidly release Taxol and therefore induce cell death only upon targeted cell internalization. Furthermore, the acidic microenvironment of most tumors could enhance the release of Taxol and dye from the nanoparticle into the tumor to facilitate the monitoring of tumor regression by MR and optical imaging. Also, by modifying the targeting moiety of the theranostic IONP's surface, other carcinomas may be targeted, while obtaining important spatiotemporal information for clinical decision making.

For in vivo imaging applications, nanoparticles with excitation and emission in the NIR region (650–900 nm) are needed for deep tissue fluorescence imaging.[17] Towards this end, we encapsulated a NIR dialkylcarbocyanine dye (DiR, excitation/emission: 751/780 nm) into the carboxylated (**2**-DiR) and folate-conjugated (**4**-DiR) IONPs, following the same synthetic protocol described for the synthesis of IONPs **2** and **4**. UV–Vis studies corroborated the presence of the NIR DiR dye within the nanoparticle's PAA coating (see Supporting Information 8b). To demonstrate the targeting capability of our functional NIR and folate-derivatized IONP (**4**-DiR) to folate-receptor-expressing cells and eventually assess their intracellular activity, we incubated A549 lung carcinoma cells with the (**4**-DiR) nanoparticle and imaged the cells using fluorescence imaging techniques.

In these studies, A549 cells (10 000 cells) were treated with either DiR-carrying carboxylated (**2**-DiR) or DiR-carrying folate-conjugated (**4**-DiR) IONPs (1.1 mg mL^{-1}) for 3 h. Next, the cells were washed with PBS and detached with trypsin. After centrifugation, the resulting cell pellets were simultaneously imaged using an indocyanine green (ICG) filter. No cell-associated NIR fluorescence was observed in cells treated with the carboxylated (**2**-DiR) nanoparticles (see Supporting Information 13A). In contrast, a dose-dependent cell-associated DiR fluorescence was observed in cells treated with the folate-conjugated (**4**-DiR) nanoparticles (see Supporting Information 13B). Since the cells were extensively washed with PBS before imaging and considering the confocal microscopy results shown in Figure 3, it is plausible that the cells have internalized the (**4**-DiR) nanoparticles via folate-receptor-mediated endocytosis, thus endowing these cells with NIR fluorescence. To further confirm the association of these nanoparticles with folate-expressing A549 carcinoma cells, the cell pellets were resuspended in PBS and their fluorescence emission and MRI signal (T_2 relaxation time) were recorded. As expected, an increase in fluorescence emission intensity and decrease in magnetic relaxivity (T_2) was observed from the corresponding suspension of the cell pellets (Table 2). No fluorescence emission or T_2 changes were observed in H9c2 cardiomyocytes treated with **4**-DiR. Therefore, these results indicate that our targeted multimodal nanoparticles can simultaneously allow the NIR fluorescence and MR imaging of folate-receptor-expressing cells.

To further assess the utility of the multimodal nanoparticle **4** encapsulating either DiI (**4**-DiI) or DiR (**4**-DiR), fluorescence and MRI studies were performed. First, phantoms containing both nanoparticles in PBS were taken using a dedicated optical imaging animal scanner (Maestro, CIR, Woburn, MA). Results indicated the potential use of the **4**-DiR nanoparticle for NIR imaging, even in a nanoparticle suspension containing both **4**-DiI and **4**-DiR IONPs (see Supporting Information 14A–E). These results are important as they point to the possibility of simultaneously imaging both nanoparticles, which could be utilized in the imaging of two different targets in in vivo experiments (e.g., two different cell populations). Furthermore, MRI studies of **4**-DiI and **4**-DiR nanoparticle dilutions (see Supporting Information 15) using a 4.7T MRI scanner (Bruker, Bellerica MA) further demonstrated the ability of these IONPs to behave as sensitive MRI contrast agents.

3. Conclusions

In conclusion, we introduce a new method to synthesize multimodal and theranostic PAA-IONPs for the potential in vivo target-specific detection and treatment of tumors. Our novel IONPs are biocompatible and biodegradable, as they are synthesized from biodegradable and biocompatible components. These functional IONPs are stable in aqueous buffered solutions, possess good cellular targeting ability, and their simple synthesis process is amenable to scale-up. In addition, this method can easily be used to generate libraries of targeted theranostic nanoparticles with different targeting ligands or encapsulated agents, and even include different metallic cores. Furthermore, the drug-encapsulating IONPs when conjugated with folic acid (using click chemistry) provide targeted drug delivery to cancer cells that overexpress the folate receptor, while avoiding normal cells that do not overexpress this receptor. We anticipate that these multimodal (magnetic and fluorescent) and multifunctional (imaging and therapeutic) IONPs will open many exciting opportunities for the targeted delivery of therapeutic agents to tumors. In addition, the dual optical and magnetic properties of the synthesized nanoparticles will allow for the dual fluorescence- and MR-based imaging and monitoring of drug efficacy. All these positive attributes make the functional IONPs a promising drug delivery vehicle for further in vivo evaluation.

Table 2. Determination of fluorescence emission intensity [a. u.] and magnetic relaxivity (T_2) of IONP-(**4**-DiR)-treated cells (A549) in PBS.

A549 Cell pellets	Cells only	Cells + 20 μL IONPs	Cells + 40 μL IONPs	Cells + 60 μL IONPs	Cells + 80 μL IONPs
Fluorescence Emission ($\times 10^5$)	0.0	1.7	2.0	2.4	2.7
T_2 [ms]	2 000	165	126	101	78

© 2009 Wiley-VCH Verlag GmbH & Co. KGaA, Weinheim

NANO MICRO small

4. Experimental Section

*Synthesis of PAA-IONPs (**1**):* For the water-based, step-wise synthesis of PAA-IONPs, three solutions were prepared: an iron salt solution (0.62 g of $FeCl_3 \cdot 6H_2O$ and 0.32 g of $FeCl_2 \cdot 4H_2O$ in dilute HCl solution (100 μL of 12 N HCl in 2.0 mL H_2O)); an alkaline solution (1.8 mL of 30% NH_4OH solution in 15 mL of N_2-purged deionized (DI) water); and a stabilizing agent solution (820 mg of PAA in 5 mL of DI water). To synthesize the PAA-IONP, the iron salt solution was added to the alkaline solution under vigorous stirring. The resulting dark suspension of IONPs was stirred for approximately 30 s before addition of the stabilizing agent solution and stirred for 1 h. The resulting suspension of PAA-IONPs was then centrifuged at 4 000 rpm for 30 min and the supernatant was washed three times with DI water to remove free PAA and other unreacted reagents using an amicon 8200 cell (Millipore ultra-filtration membrane YM–30 k). Finally, the PAA-IONP suspension was purified using a magnetic column, washed with PBS (pH 7.4) and concentrated using the amicon 8200 cell system. The iron concentration and magnetic relaxation of the PAA-IONPs was determined as previously reported.[18] The successful coating of the IONPs with PAA was confirmed by the presence of a negative zeta-potential ($\zeta = -48$ mV) and the characteristic acid carbonyl bands on the FTIR spectroscopic analysis of the nanoparticles (see Supporting Information 1 and 5).

*Synthesis of propargylated IONPs (**3**); Carbodiimide chemistry:* To a suspension of PAA-IONP (**1**) (45 mg Fe) in 2-(*N*-morpholino) ethanesulfonic acid (MES) buffer (26 mL, pH 6), a solution of (1-ethyl-3-[3-dimethylaminopropyl]carbodiimide hydrochloride) (EDC) (87 mg, 10 mmol) and *N*-hydroxy succinimide (NHS) (52 mg, 10 mmol) in MES buffer (2 mL) was added and incubated for 3 min. To the resulting reaction mixture, propargyl amine (25 mg, 10 mmol) in DMF (0.5 mL) was added drop-wise and incubated for 5 h at room temperature. The resulting reaction mixture was then purified using a magnetic column and then using amicon 8200 cell (Millipore ultra-filtration membrane YM–30 k) to remove unreacted propargyl chloride and other unreacted reagents and kept in PBS at 4 °C. FTIR data analysis (see Supporting Information 6) confirms the completion and success of the conjugation.

*General procedure for dye-encapsulated functional IONPs (**2**, **4**); Modified solvent diffusion method:* To a suspension of IONPs (4.5 mL, [Fe] = 1.1 mg mL^{-1}) in PBS, a solution of the corresponding dialkylcarbocyanine fluorescent dyes (DiI or DiR, 0.1 μg μL^{-1}) in DMF was added drop-wise at room temperature with continuous stirring at 1 000 rpm. The resulting dye-encapsulated IONPs were purified using a magnetic column and then dialyzed (using 6–8 K molecular weight cut-off dialysis bag) three times against DI water and finally against PBS solution. The successful encapsulation of the corresponding dye (DiI or DiR) on the PAA-IONPs was confirmed by UV–Vis spectrophotometric measurements (see Supporting Information 6a and b). In addition, when these nanoparticles were functionalized with folate, the presence of both folate- and dye-encapsulated groups were assessed by UV–Vis (see Supporting Information 9a) and fluorescence (see Supporting Information 9b) spectrometry.

*Procedure for the co-encapsulation of Paclitaxel and DiI into IONPs (**5**):* A solution containing paclitaxel (5 μL, 0.05 μg μL^{-1}) and DiI dye (5 μL, 0.1 μg μL^{-1}) in 500 μL DMF was used and the same modified solvent diffusion method was followed as described above. The presence of Taxol in the IONPs (**5**) was confirmed by using fluorescence spectrophotometry (see Supporting Information 10).

*Synthesis of **3a**; Folate conjugation using click chemistry:* To a suspension of propargylated IONPs **3** (13 mg Fe) in bicarbonate buffer (pH 8.5), a catalytic amount of CuI (0.06 μg, 3×10^{-10} mmol) was added for a total volume of 125 μL of bicarbonate buffer and vortexed for 30 s. Then, a solution of azide-functionalized folic acid (**7**, see Supporting Information 2, 0.003 g, 6×10^{-2} mmol) in dimethyl sulfoxide (DMSO) was added and incubated at room temperature for 12 h. The final reaction mixture was purified by using a magnetic column and by dialysis using 6–8 K molecular weight cut-off dialysis bag, against DI water first and finally with a PBS solution. The purified functional IONPs were stored at 4 °C until further use. The successful conjugation of folic acid with PAA-IONPs was confirmed by UV–Vis (see Supporting Information 7a) and fluorescence (see Supporting Information 7b) spectrophotometric measurements.

Cell culture and cell viability studies; MTT assay: The lung carcinoma cells (A549) and cardiomyocytes (H9c2) were obtained from ATCC, USA. Lung carcinomas were grown in Kaighn's modification of Ham's F12 medium (F12K, Cellgro), supplemented with 5% fetal bovine serum (heat-inactivated FBS, Cellgro), L-glutamine, streptomycin, amphotericin B, and sodium bicarbonate. The cells were maintained at 37 °C, 5% CO_2 in a humidified incubator. Cardiomyocyte cells were grown in Eagle's Minimal Essential medium supplemented with 10% fetal bovine serum, sodium pyruvate, L-glutamine, penicillin, streptomycin, amphoricin B, and sodium bicarbonate. For MTT assay, lung carcinoma and cardiomyocyte cells (2 500 cells per well) were seeded in 96-well plates, and were incubated with the IONPs for 3 h at 37 °C. Then, each well was washed three times with 1X PBS and treated with 20 μL MTT (5 μg μL^{-1}, 3-(4,5-dimethylthiazol-2-yl)-2,5-diphenyltetrazo-lium bromide, Sigma-Aldrich) for 2 h. The resulting formazan crystals were dissolved in acidified isopropanol (0.1 N HCl) and the absorbance was recoded at 570 and 750 nm (background) using a Synergy HT multidetection microplate reader (Biotek). These experiments were performed in triplicate.

Cellular internalization; confocal microscopy and IVIS experiments: Zeiss LSM 510 confocal and Zeiss Axiovert 200 epifluorescence microscopes were used to assess the uptake of folate-derivatized IONPs by the human lung carcinoma (A549) cell line. Specifically, A549 cells (10 000) were incubated with the corresponding IONPs preparation (1.1 mg mL^{-1}) for 3 h in a humidified incubator (37 °C, 5% CO_2). Subsequently, the cells were thoroughly washed three times with 1X PBS and fixed with 10% formalin solution. Nuclear staining with 4′,6-diamidino-2-phenylindole (DAPI) was performed as recommended by the supplier. Then, multiple confocal images were obtained, achieving a representative view of the cell–IONPs interaction. For the In Vivo Imaging System (IVIS) analysis, 10 000 lung carcinoma cells were incubated for 3 h with the corresponding IONPs and the supernatant was collected in eppendorf tubes. Cells were thoroughly washed with 1X PBS and detached, as stated above. The resulting

 © 2009 Wiley-VCH Verlag GmbH & Co. KGaA, Weinheim

pellets were resuspended in 1 mL culture media. All eppendorf tubes were examined simultaneously on a Xenogen IVIS system, using the ICG filter for DiR dye. All experiments were performed in triplicate.

In vitro drug/dye release: The in vitro drug/dye release studies were carried out using a dynamic dialysis technique at 37 °C. Briefly, 100 μL of IONPs (**5**) are incubated with a porcine liver esterase (20 μL) inside a dialysis bag (MWCO 6 000–8 000), which is then placed in a PBS solution (pH 7.4). The amount of guest (dye or drug) molecules released from the nanoparticle into the PBS solution was determined at regular time intervals by taking 1-mL aliquots from the PBS solution and measuring the fluorescence intensity at 581 nm for DiI and 375 nm for Taxol. The concentration of the either dye or drug was calculated using a standard calibration curve. The cumulative fraction of release versus time was calculated using the following equation

$$\text{Cumulative release } (\%) = \frac{[\text{guest}]_t}{[\text{guest}]_{\text{total}}} \cdot 100\% \quad (1)$$

where $[\text{guest}]_t$ is the amount of guest released at time t and $[\text{guest}]_{\text{total}}$ is the total guest present in the guest encapsulated IONPs.

Acknowledgements

This work was supported by NIH grants CA101781 and GM084331 to JMP. We thank Dr. Korey Sorge at Florida Atlantic University for SQUID studies. Technical services provided by the MSKCC Small Imaging Core Facility from NIH Small Animal Imaging Research Program (SAIRP) Grant No. R24 CA83084 and NIH Grant No. P30 CA08748 are acknowledged. This work was also supported in part by R25 CA096945-05 (JG).

[1] a) J. R. McCarthy, K. A. Kelly, E. Y. Sun, R. Weissleder, *Nanomedicine* **2007**, *2*, 153-L 167; b) A. K. Gupta, M. Gupta, *Biomaterials* **2005**, *26*, 3995–4021.

[2] N. Nasongkla, E. Bey, J. Ren, H. Ai, C. Khemtong, J. S. Guthi, S. F. Chin, A. D. Sherry, D. A. Boothman, J. Gao, *Nano Lett.* **2006**, *6*, 2427–2430.

[3] a) M. Lewin, N. Carlesso, C. H. Tung, X. W. Tang, D. Cory, D. T. Scadden, R. Weissleder, *Nat. Biotechnol.* **2000**, *18*, 410-L 414; b) L. Josephson, M. F. Kircher, U. Mahmood, Y. Tang, R. Weissleder, *Bioconjugate Chem.* **2002**, *13*, 554-L 560; c) K. C. Weng, C. O. Noble, B. Papahadjopoulos-Sternberg, F. F. Chen, D. C. Drummond, D. B. Kirpotin, D. Wang, Y. K. Hom, B. Hann, J. W. Park, *Nano Lett.* **2008**, *8*, 2851–2857.

[4] a) J. H. Choi, F. T. Nguyen, P. W. Barone, D. A. Heller, A. E. Moll, D. Patel, S. A. Boppart, M. S. Strano, *Nano Lett.* **2007**, *7*, 861-L 867; b) W. J. Mulder, R. Koole, R. J. Brandwijk, G. Storm, P. T. Chin, G. J. Strijkers, C. de Mello Donega, K. Nicolay, A. W. Griffioen, *Nano Lett.* **2006**, *6*, 1–6.

[5] M. K. Yu, Y. Y. Jeong, J. Park, S. Park, J. W. Kim, J. J. Min, K. Kim, S. Jon, *Angew. Chem. Int. Ed.* **2008**, *47*, 5362–5365.

[6] H. Lee, M. K. Yu, S. Park, S. Moon, J. J. Min, Y. Y. Jeong, H. W. Kang, S. Jon, *J. Am. Chem. Soc.* **2007**, *129*, 12739–12745.

[7] H. Lee, E. Lee, K. Kim do, N. K. Jang, Y. Y. Jeong, S. Jon, *J. Am. Chem. Soc.* **2006**, *128*, 7383–7389.

[8] S. Peng, C. Wang, J. Xie, S. Sun, *J. Am. Chem. Soc.* **2006**, *128*, 10676–10677.

[9] a) J. R. McCarthy, J. M. Perez, C. Bruckner, R. Weissleder, *Nano Lett.* **2005**, *5*, 2552-L 2556; b) B. S. Packard, D. E. Wolf, *Biochemistry* **1985**, *24*, 5176–5181.

[10] a) E. Y. Sun, L. Josephson, R. Weissleder, *Mol. Imaging* **2006**, *5*, 122-L 128; b) H. C. Kolb, M. G. Finn, K. B. Sharpless, *Angew. Chem. Int. Ed.* **2001**, *40*, 2004-L 2021; c) M. A. White, J. A. Johnson, J. T. Koberstein, N. J. Turro, *J. Am. Chem. Soc.* **2006**, *128*, 11356–11357.

[11] a) S. Santra, B. Liesenfeld, D. Dutta, D. Chatel, C. D. Batich, W. Tan, B. M. Moudgil, R. A. Mericle, *J. Nanosci. Nanotechnol.* **2005**, *5*, 899–904; b) K. Riebeseel, E. Biedermann, R. Lser, N. Breiter, R. Hanselmann, R. Mlhaupt, C. Unger, F. Kratz, *Bioconjugate Chem.* **2002**, *13*, 773–785.

[12] M. Shi, J. H. Wosnick, K. Ho, A. Keating, M. S. Shoichet, *Angew. Chem. Int. Ed.* **2007**, *46*, 6126–6131.

[13] a) A. M. Koch, F. Reynolds, M. F. Kircher, H. P. Merkle, R. Weissleder, L. Josephson, *Bioconjugate Chem.* **2003**, *14*, 1115-L 1121; b) T. Shen, R. Weissleder, M. Papisov, A. Bogdanov, Jr., T. J. Brady, *Magn. Reson. Med.* **1993**, *29*, 599–604.

[14] N. Parker, M. J. Turk, E. Westrick, J. D. Lewis, P. S. Low, C. P. Leamon, *Anal. Biochem.* **2005**, *338*, 284–293.

[15] H. Yuan, J. Miao, Y. Z. Du, J. You, F. Q. Hu, S. Zeng, *Int. J. Pharm.* **2008**, *348*, 137–145.

[16] M. E. Nelson, N. A. Loktionova, A. E. Pegg, R. C. Moschel, *J. Med. Chem.* **2004**, *47*, 3887–3891.

[17] R. Weissleder, V. Ntziachristos, *Nat. Med.* **2003**, *9*, 123–128.

[18] L. Josephson, C. H. Tung, A. Moore, R. Weissleder, *Bioconjugate Chem.* **1999**, *10*, 186–191.

Received: March 4, 2009
Published online: April 20, 2009

 © 2009 Wiley-VCH Verlag GmbH & Co. KGaA, Weinheim